Exploring Dissolved Organic Carbon Variations in a High Elevation Tropical Peatland Ecosystem: Cerro de la Muerte, Costa Rica

Sánchez-Murillo Ricardo [1,2]*, Gastezzi-Arias Paola [3], Sánchez-Gutiérrez Rolando [2], Esquivel-Hernández Germain [2], Pérez-Salazar Roy [4] and Poca María [5]

[1] Department of Earth and Environmental Sciences, University of Texas at Arlington, Arlington, TX, United States, [2] Stable Isotopes Research Group and Water Resources Management Laboratory, Chemistry School, Universidad Nacional, Heredia, Costa Rica, [3] Doctorado en Ciencias Naturales Para el Desarrollo Costa Rica (DOCINADE), Instituto Tecnológico de Costa Rica and Laboratorio de Vida Silvestre y Salud, Vicerrectoría de Investigación de la Universidad Estatal a Distancia, San José, Costa Rica, [4] Laboratorio de Gestión de Desechos y Aguas Residuales, Escuela de Química, Universidad Nacional, Heredia, Costa Rica, [5] Instituto de Matemática Aplicada San Luis, Universidad Nacional de San Luis, Consejo Nacional de Investigaciones Científicas y Técnicas (CONICET), Grupo de Estudios Ambientales, San Luis, Argentina

Tropical peatlands are distributed mainly in coastal lowlands; however high elevation regions exhibit a large prevalence of small and fragmented peatlands that are mostly understudied. Artificial drainage of peatlands to expand the area of cattle farming, horticulture, and urbanization is increasing carbon losses to the atmosphere and streams worldwide. Here, we present an exploratory characterization of dissolved carbon optical properties in ombrotrophic peat bogs of the Talamanca range of Costa Rica, across an altitudinal gradient (2,400–3,100 m a.s.l.) during the rainy season. Dissolved organic matter (DOM) sources and decomposition processes were evaluated in the light of dissolved organic and inorganic carbon (DOC and DIC), optical properties, and major water chemistry. DOC concentrations ranged from 0.2 up to 47.0 mg/L. DIC concentrations were below 2 mg/L and $\delta^{13}C_{DIC}$ values indicated a mixture between soil organic matter, CO_2 in soil water, and to a lesser degree DIC derived from bacterial CO_2. Absolute fluorescence intensity of humic-like peaks was 6–7 times greater than fresh-like peaks across all sites. Fluorescence peak ratios coupled with the biological and humification indexes point to a greater relative contribution of recalcitrant soil-derived DOM. Excitation/Emission matrices denoted a high prevalence of humic and fulvic acids in the peat bogs, with moderate intensities in soluble microbial by-products-like and aromatic protein regions at three sites. Our data provides a baseline to underpin tropical carbon dynamics across high elevation peatlands.

Keywords: tropical high elevation peatlands, dissolved organic carbon, optical properties, carbon storage, climate variability

INTRODUCTION

Peatlands are a type of wetlands which are defined as having saturated soils, dense vegetation, anoxic conditions, and large deposits of partially decomposed organic plant material or peat (i.e., soil organic matter 30–50% in a 20–40 cm profile) (Yu, 2011; Page and Baird, 2016; Bourgeau-Chavez et al., 2018; Villa et al., 2019; Ribeiro et al., 2021). Peat accumulates as a result of the long-term imbalance between carbon production and decomposition (Hapsari et al., 2017; Bourgeau-Chavez et al., 2018). Tropical peatlands play an important role in the global carbon cycle due to their immense storage capacity, preserving between 469 and 694 Gt C in a relatively small area (90–170 Mha), equivalent to one third of the total global carbon pool (Müller et al., 2015; Gumbricht et al., 2017; Hapsari et al., 2017).

Tropical peatlands are distributed mainly in the river deltas and coastal plains, although mountainous areas also contain many small and fragmented peatlands (Hribljan et al., 2016; Hapsari et al., 2017; Lourençato et al., 2017; Silva et al., 2019). Mountainous peatlands offer a broad spectrum of ecosystem services, such as regulating stream discharge and lowland flooding, sediment and nutrient retention, carbon storage, and are home of a large number of endemic species (Kimmel and Mander, 2010; Ribeiro et al., 2021). Artificial peatland drainage may result in the net loss of the C storage function and in a large release of greenhouse gases to the atmosphere (e.g., CO, CO_2, and CH_4; Page and Baird, 2016).

Despite the recent research interest and new data available about the key role of peatland worldwide, the carbon quality (i.e., humic and fulvic acids, protein and microbial-like materials) and ecohydrological functioning of high elevation peatlands remain understudied in the tropics mainly due to sampling sites accessibility during the rainy season (Gandois et al., 2014; Hribljan et al., 2016; Pesántez et al., 2018).

Tropical peatlands, especially those in freshwater swamp forests, are mostly fed by partially decayed organic matter, which is often composed of recalcitrant plant litter that decomposes under acidic and anaerobic conditions at particularly slow rates (Bourgeau-Chavez et al., 2018; Cooper et al., 2019; Leng et al., 2019). In general, the decomposition process is regulated by local precipitation amount and seasonal perched water tables, which determine the shape and extent of the peatland surface and specify the ultimate stable morphology, and hence the carbon storage, within the adjacent network of rivers or canals (Villa et al., 2019). Therefore, a substantial reduction in rainfall may alter the peat surface dynamics, which in combination to warm temperatures may lead to higher rates of mineralization and degassing of the partly decomposed organic matter within peatlands (Li et al., 2007; Fenner and Freeman, 2011; Lourençato et al., 2017; Leng et al., 2019).

Dissolved organic carbon (DOC) in peatlands can originate from several sources, including recent photosynthetic by-products, decomposition, and dissolution products within the peat column (Moore et al., 2013). DOC in peatlands reflects the carbon source characteristics and transformations, namely vegetation, peat/soil respiration, and microbial activity (Cooper

et al., 2010; Marx et al., 2017). The advent of cost-effective laboratory techniques, such as absorbance and fluorescence, has promoted the use of dissolved organic matter (DOM) as an environmental tracer in many ecosystems (Cook et al., 2017; Dalmagro et al., 2017; Park and Snyder, 2018; Chaves et al., 2020).
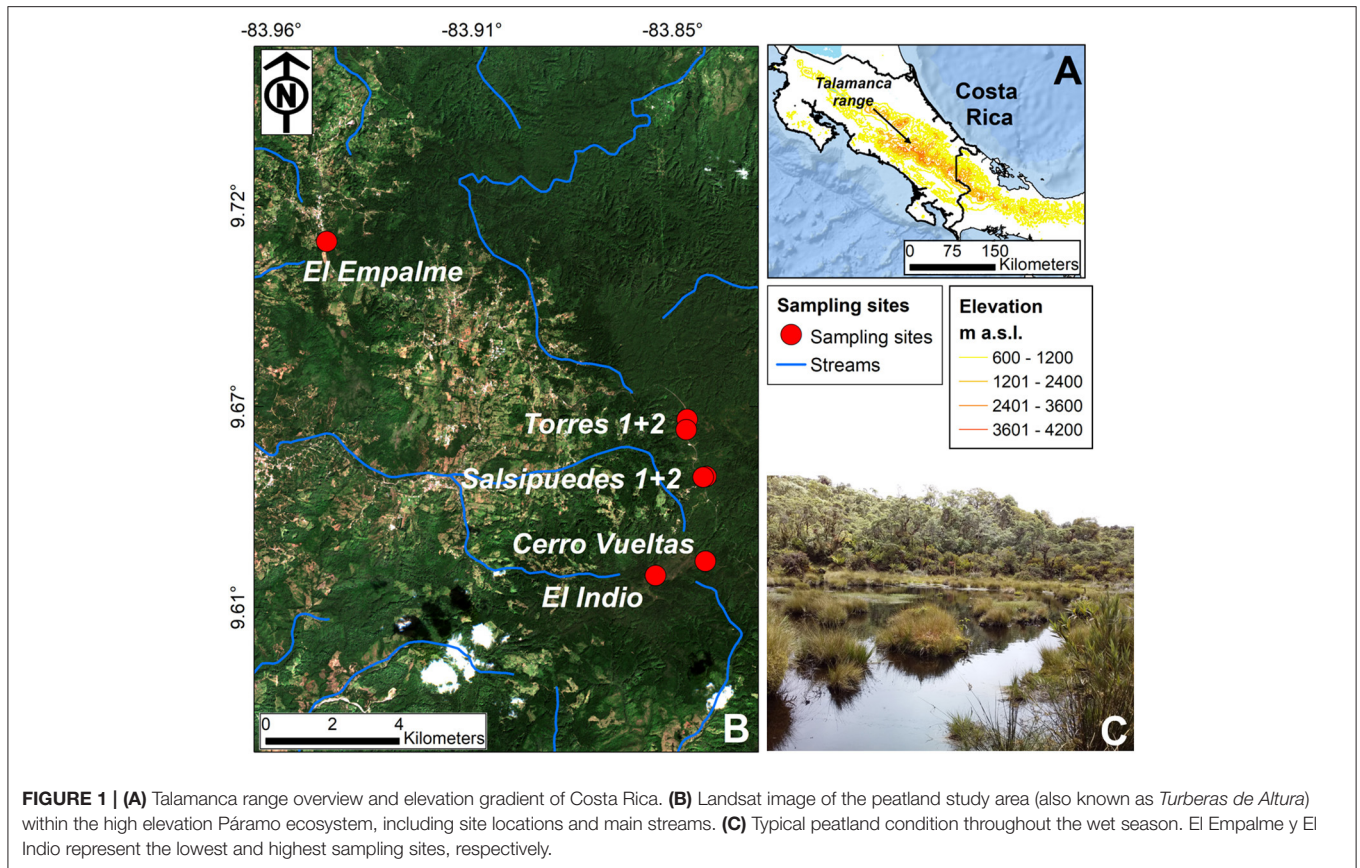
Contrary to boreal and temperate peatlands where seasons control freezing and thawing, as well as microbial activity, DOM composition in wet tropical peatlands is mainly shaped by the large rainfall variability (Bispo et al., 2016). For example, during drought periods perched water tables are lowered, which in turn produces oxic conditions and stimulates phenol oxidase enzymes, therefore reducing the overall concentration of polyphenolics and their inhibitory effect on DOC decomposition via hydrolase enzymes (Ritson et al., 2017 and references therein).

Natural drainage of these systems are then important pathways for terrestrial carbon export in the forms of DOC, particulate organic carbon (POC), and dissolved inorganic carbon (DIC) (Kiew et al., 2018; Waldron et al., 2019). In some regions such as Southeast Asia, however, increasing human disturbances of tropical peatlands by fire and artificial drainage for agriculture have resulted in emissions of stored carbon at very fast rates (Page et al., 2002; Couwenberg et al., 2010; Itoh et al., 2017; Cooper et al., 2019). Therefore, an assessment of the stability of these tropical carbon stocks across different ecosystems is necessary to estimate the potential effects of increasing anthropogenic disturbances (Drake et al., 2019; Ribeiro et al., 2021).

In Central America, examples of these high mountain peatlands or bogs, known as "Turberas de Altura" (Gómez, 1986) are found between 2,400 and 3,100 m a.s.l. along the continental divide of the Talamanca range in Costa Rica (Brak et al., 2005; Corrales Ulate, 2018; **Figure 1**). These peat-forming bogs are restricted to small and poorly drained depressions subject to seasonal flooding (during the rainy season from May to November; Amador, 1998), and with an area just over 235 ha (Jiménez, 2016). In this region, soil organic carbon ranged from 31 up to 43% in the first 50 cm of the soil profile (Corrales Ulate, 2018). Given the limited information and current anthropogenic pressure across mountainous ecosystems of Costa Rica (Corrales Ulate, 2018; Stan and Sanchez-Azofeifa, 2019), there is an urgent need to understand the high elevation peatlands potential for carbon storage and export in a changing climate and land use scenario.

Here we present an exploratory characterization of DOM optical properties in peat bogs of the Talamanca range across an altitudinal transect (from 2,400 to 3,100 m a.s.l.) during a complete wet season. DOM sources and decomposition processes were evaluated with respect to DOC concentrations, optical properties, and major water chemistry composition. We hypothesize that water depth, temperature seasonality, and solar radiation exert a large control on DOC properties within the high elevation peat bogs.

Our data provides a baseline to underpin carbon dynamics of high mountain peatlands in the Central American region, which in turn may help to allocate efforts and resources for conservation strategies under the Payment for Environmental Services (i.e., payment for forest conservation and ecosystem services) scheme

FIGURE 1 | (A) Talamanca range overview and elevation gradient of Costa Rica. **(B)** Landsat image of the peatland study area (also known as *Turberas de Altura*) within the high elevation Páramo ecosystem, including site locations and main streams. **(C)** Typical peatland condition throughout the wet season. El Empalme y El Indio represent the lowest and highest sampling sites, respectively.

(Arriagada et al., 2015; Berbés-Blázquez et al., 2017; Wallbott et al., 2019) across these sensitive ecosystems.

STUDY AREA

Study sites are located in the Pacific domain of the Talamanca range, Costa Rica (**Figure 1A**). During the last glacial maximum, this region was glaciated with an ice cap of roughly 5 km^2; the latter is evidenced by smoothed, grooved, and channeled andesite bedrock surfaces (Lachniet and Seltzer, 2002). Long-term weathering has facilitated the formation of concave landforms, which in turn facilitates water accumulation in such topographic depressions. These peat-forming bogs are found between 2,400 and 3,100 m a.s.l. and cover small areas (up to 0.5 ha), whereby surface drainage is relatively poor.

Meteorological conditions across this gradient are fairly similar throughout the wet season. Water table fluctuation is mostly controlled by the seasonal rainfall input with ∼80% of the annual rainfall falling between May and November (**Figure 2**). The greatest variation in temperature and relative humidity was observed during the dry season (December–April, **Figure 2**). During the wet season, rainfall input leads to saturated soils and anoxic conditions, peat accumulation, and water acidification. In general, solar radiation effective hours range from 4 to 8 per day during the wet and dry seasons, respectively. More than 100 species of forbs, grasses, and sedges have been reported

from the Páramo peat bogs of Costa Rica (Gómez, 1986). **Table 1** summarizes the main vegetation and morphological characteristics of the study sites obtained from field observations.

METHODS

Sample Collection

Seven highland peat bogs were studied during the 2019 wet season (**Figure 1B**) (7 monthly sampling campaigns). Peat bog samples for the analysis of DOC/DIC, optical properties, stable isotopes, and major ions were collected during the wet season, from the beginning of May through the end of November, 2019. Site accessibility and water storage within the peatlands were key factors to select the sites (**Figure 1C**).

Carbon and major ions samples were collected on monthly basis in pre-cleaned 250 mL glass amber bottles (including oven-heated treatment) covered with aluminum foil to prevent samples from solar/light radiation. Stable isotopes samples were collected in 50 mL pre-cleaned HDPE bottles with plastic inserts to prevent evaporation. Sampling bottles were rinsed at least three times with the peatland water before collection. Rainfall monitoring for stable isotopes analysis was conducted using a passive Palmex collector (daily collection; $N = 103$) (Gröning et al., 2012; Esquivel-Hernández et al., 2021). During transportation and after filtering, all samples were stored at 5°C until analysis. Electrical conductivity (EC, µS/cm), pH, turbidity (NTU), and fDOM

FIGURE 2 | Study area meteorological conditions during 2019. Black bars denote rainfall in mm/h. Red and blue lines correspond to hourly ambient temperature and relative humidity fraction, respectively.
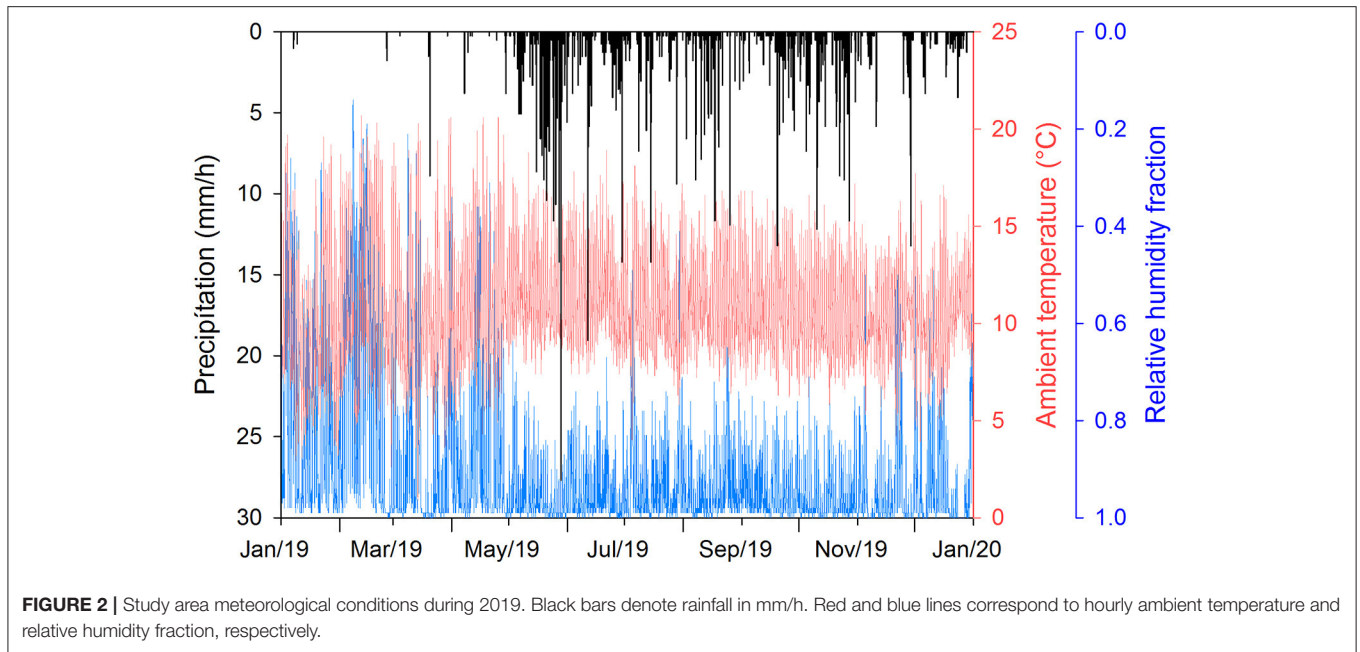
TABLE 1 | Summary of main vegetation and morphological characteristics of the study sites.

Study sites	Elevation (m a.s.l.)	Main characteristics
El Empalme	2,400	This site presents heterogeneous vegetation of secondary forest mixed with pasture and shrubs, due to human activities (i.e., cattle farms, crops). In the rainy season, this peat bog forms small intermittent ponds of little depth (water column depth <60 cm). In the dry season, the soils remain between field capacity and saturation. Tadpoles and aquatic insects have been observed in these ponds.
Torres 1-2	2,600	The vegetation is represented by a continuous strip of montane forest with scattered arborescent ferns, Iridaceae, Ciperaceae, and mosses covering the ground. These peat bogs are permanent and shallow (water column depth <60 cm) with visible draining channels covered by herbaceous vegetation. In the dry season, the soils remain between field capacity and saturation.
Salsipuedes 1-2	2,800	Vegetation is characterized by montane forest, with tree ferns, mosses, Ciperaceae (grass-like), and bromeliads. These peat bogs are comprised of small, shallow lagoons during the rainy season. In the dry season, the soils remain between field capacity and saturation.
Cerro Vueltas and Indio	3,100	The vegetation is represented by secondary subalpine forest, and Páramo grasslands, with the presence of arborescent ferns, mosses, bromeliads, and Chusquea. Both peat bogs are mostly seasonal. In the dry season, the soils remain between field capacity and saturation.

(QSU; quinine sulfate units) were recorded using a pre-calibrated multi-parameter sonde EXO1 (YSI Inc., USA) immediately after sample arrival at the laboratory.

Water Stable Isotopes Analysis

Samples were analyzed at the Stable Isotopes Research Group laboratory at the Universidad Nacional (Heredia, Costa Rica) using an IWA-45EP water analyzer (Los Gatos Research, Inc., California, USA) with a precision of $\pm 0.5‰$ for δ^2H and $\pm 0.1‰$ for $\delta^{18}O$ (1σ; 8 injections). Stable isotope compositions are expressed as $\delta^{18}O$ or $\delta^2H = (Rs/Rstd – 1)\cdot 1,000$, where R is the $^{18}O/^{16}O$ or $^2H/^1H$ ratio in a sample (s) or standard (std) and reported in the delta-notation (‰) relative to V-SMOW/SLAP

scale. The instrument accuracy was assessed with a combination of in-house and primary international water standards (SMOW and SLAP). Deuterium excess was calculated as d-excess $= \delta^2H – 8\cdot\delta^{18}O$ (Dansgaard, 1964).

DOC Analysis

DOC contents were measured using a TOC analyzer (Aurora 1030W, OI Analytical) following the Heated-Persulfate Oxidation Method 5310C (APHA AWWA, 2005). Each water sample was filtered using 0.45 μm PTFE filter into 100 mL pre-cleaned vials. A standard curve was conducted using six calibration solutions (i.e., stock solution of anhydrous primary-standard-grade potassium biphthalate, $C_8H_5KO_4$) ranging from

0 to 100 mg C L^{-1} (Method SM5310 C; APHA AWWA, 2005). The quantification and detection limits were 0.05 and 0.03 mg C L^{-1} (Sánchez-Murillo et al., 2019).

$\delta^{13}C_{DIC}$ Analysis and Total Alkalinity

Filtered aliquots (0.45 μm cellulose filter) (6 mL) were pipetted into Exetainer® vials. An automated DIC sample preparation system (Picarro AutoMate FX system, USA) was utilized to inject a 10% phosphoric acid solution into each sealed vial to liberate CO_2 from the sample. Additionally, a stream of dry and ultra-pure nitrogen was bubbled through the acidified solution to flush the released CO_2 from the vial headspace. The CO_2 was captured into gas sampling bags of a Picarro Liaison^{TM} Universal Interface before being analyzed using Cavity Ring Down Spectroscopy (CRDS, Picarro G2201-i). After each measurement, the instrument and the gas sampling bag were purged with fully dry and ultra-pure nitrogen between successive DIC/δ^{13}C measurements. The corresponding uncertainty for δ^{13}C in DIC is ±0.1‰ (1σ). Calibration was done using the following standards: University of McGill, Canada: CO_2 mixing ratio: 1,553 ppmv, $\delta^{13}CO_2 = -43.15‰$, Heredia's compressed air: CO_2 mixing ratio: 419.1 ppmv, $\delta^{13}CO_2 = -10.09‰$, NOAA gas standard: CO_2 mixing ratio: 394.85 ppmv, $\delta^{13}CO_2 = -8.292‰$. Stable isotope compositions are expressed as $\delta^{13}C = (Rs/Rstd - 1)\cdot1,000$, where R is the $^{13}C/^{12}C$ ratio in a sample (s) or standard (std) and reported in the delta-notation (‰) relative to VPDB scale (Craig, 1957).

The total alkalinity of each sample (reported as $CaCO_3$) was also calculated from the average CO_2 concentration measured during the isotope analysis. The CO_2 concentration measured by the CRDS was standardized against Na_2CO_3 solutions (Sigma Aldrich, >99.0%, 5–100 mg/L). These standard solutions were analyzed following the same procedure described above. Given the small volume of sample that is analyzed by this method, only those water samples with a total alkalinity >10 mg/L were quantified.

Major Ions Analysis

Major ions samples were filtered using 0.45 μm PTFE and/or PVDF filter into 5 mL HDPE pre-cleaned poly vials. Ion chromatography (Thermo Scientific ICS-5000+, CA, USA) was used to analyze lithium, ammonium, sodium, potassium, magnesium, calcium, bromide, chloride, fluoride, nitrite, nitrate, and sulfate [DL (mg/L): 0.011, 0.035, 0.64, 0.20, 0.19, 0.23, 0.50, 0.23, 0.18, 0.26, 0.22 and 0.20, respectively]; to ensure the quality of the analysis, procedural blanks and recovery standards were performed in each batch of samples.

DOC Optical Properties

The water column of these shallow wetland ponds may be completely anoxic but due to sampling constraints we were unable to confirm that water samples were kept anoxic prior to measurement of optical properties.

DOC excitation-emission matrices (EEMs) were measured (in absolute fluorescence intensity) using a FP-8300 spectrofluorometer (Jasco, Tokyo, Japan) equipped with double monochromators both at the excitation and the emission sides. Excitation wavelength were set up in the range of 200–450 nm with sequential increments of 5 nm with an integration time of 0.5 s and increments of 1 nm in the emission wavelength for the range of 280–550 nm. Spectral corrections for the EEMs were done with sample blanks that were carried out using deionized water type I in each batch of samples under the same conditions to eliminate water Raman peaks (Huguet et al., 2009).
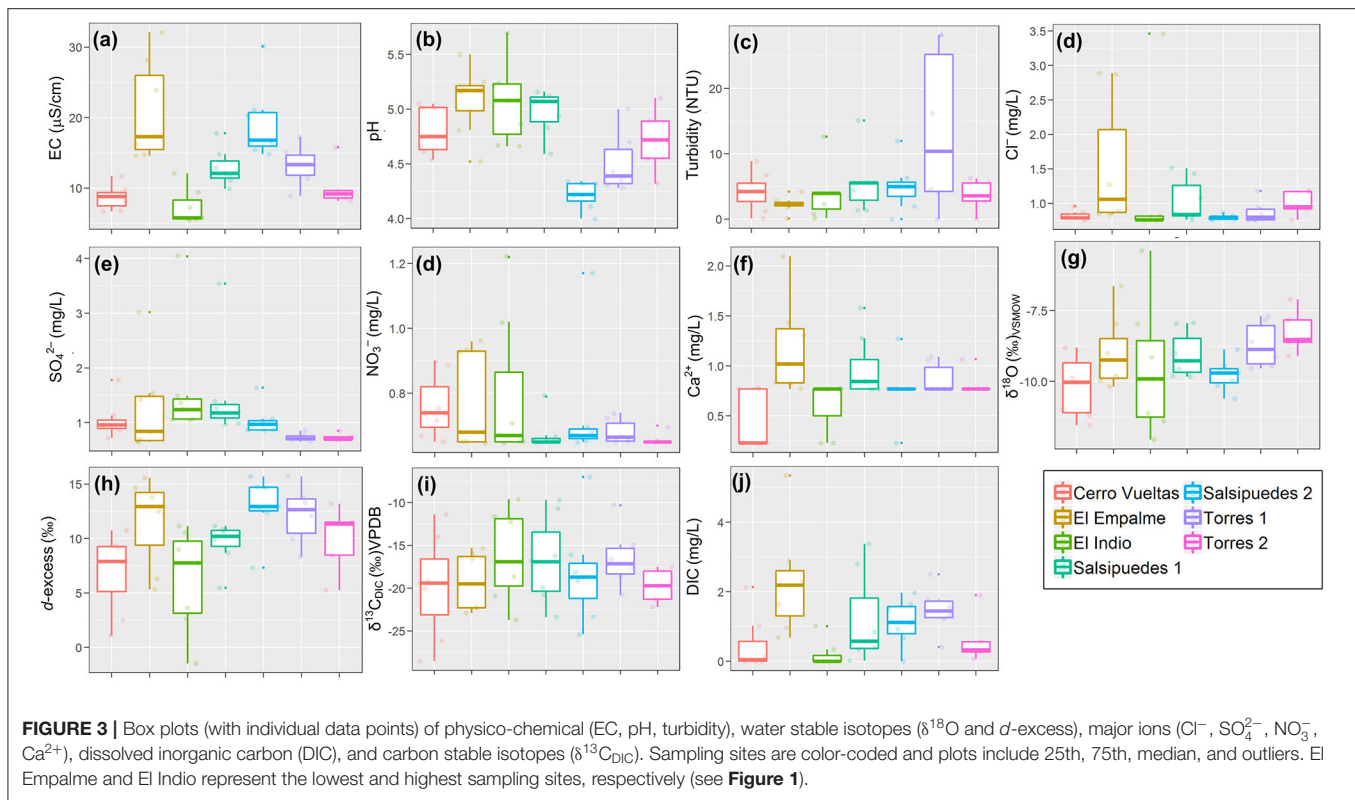
Chromophoric dissolved organic matter (DOM) absorbance at 254.7 nm (a_{254}, m^{-1}) was measured (Method 5910B; APHA AWWA, 2005) using UV-spectrophotometry (Jasco VP-750, Tokyo, Japan). For all the samples, the absorbance of a blank sample prepared with deionized water type I was measured as a spectral correction using quartz cells of 1 cm path length. EEMs diagrams are presented following Chen et al. (2003) wavelength boundaries (in absolute fluorescence intensity). It is important to highlight that the lack of a proper inner filter effect correction limited the comparative potential of our exploratory results with other studies.

Statistical and Optical and Data Analysis

EEMs were analyzed as a qualitative tool for assessing the principal sources of DOC in the water. The well-known Coble peaks (Coble, 1996) (in absolute fluorescence intensity), the fluorescence index (FI) (Mcknight et al., 2001), the humification index (HIX) (Zsolnay et al., 1998) and the autochthonous biological activity index (BIX) (Huguet et al., 2009) were calculated using the staRdom package (Pucher et al., 2019). Fluorescence measurements (including ratios) are not corrected for the strong absorption of these samples, so our results must be considered carefully in comparison with other studies. Nonetheless, the patters we observed are informative for this preliminary investigation into DOM properties in these understudied systems.

Spearman (1904) correlation coefficients and principal component analysis (PCA) were applied to further identify common parameters that are influencing dissolved carbon optical properties. Data below quantification limits (QL) were transformed to tie ranks before performing multivariate analysis (Helsel, 2012). Principal component analysis was carried out through the FactoMineR package (Lê et al., 2008), the data were scaled for unit variance in order to avoid some variables become dominant because of their intrinsic differences in units and variability; while the number of final dimensions were not constrained. In order to evaluate differences between parameters within each sampling site or sample campaign, we compute a one factor permutation test (Blair et al., 1994; Good, 2000), where the results that have been obtained by parameter (e.g., BIX) for each factor (e.g., sampling site) were shuffled 5,000 times doing a resampling procedure to estimate different means.

In addition, an exploratory correlation matrix was conducted using the corr R package (Friendly, 2002; R., Core Team, 2019; Wei and Simko, 2021). All variables exhibiting collinearity were removed prior the analysis. Only significant Spearman correlations (α = 0.05) were visualized (see **Supplementary Figure 1**).
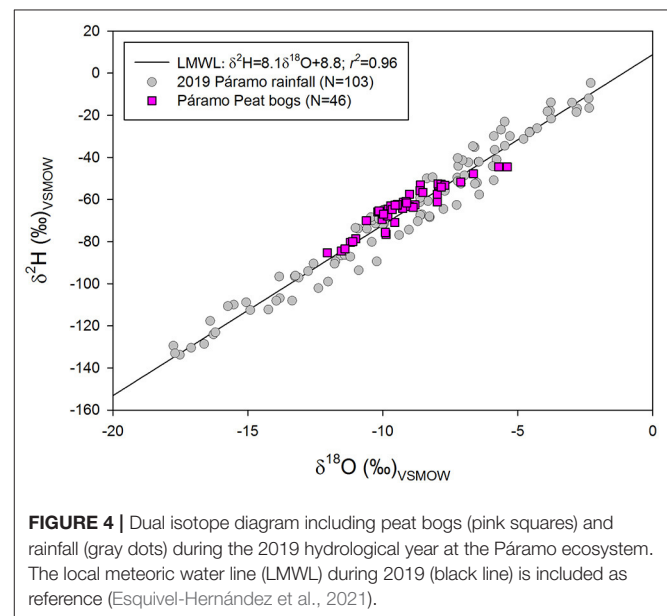
FIGURE 3 | Box plots (with individual data points) of physico-chemical (EC, pH, turbidity), water stable isotopes ($\delta^{18}O$ and d-excess), major ions (Cl^-, SO_4^{2-}, NO_3^-, Ca^{2+}), dissolved inorganic carbon (DIC), and carbon stable isotopes ($\delta^{13}C_{DIC}$). Sampling sites are color-coded and plots include 25th, 75th, median, and outliers. El Empalme and El Indio represent the lowest and highest sampling sites, respectively (see **Figure 1**).
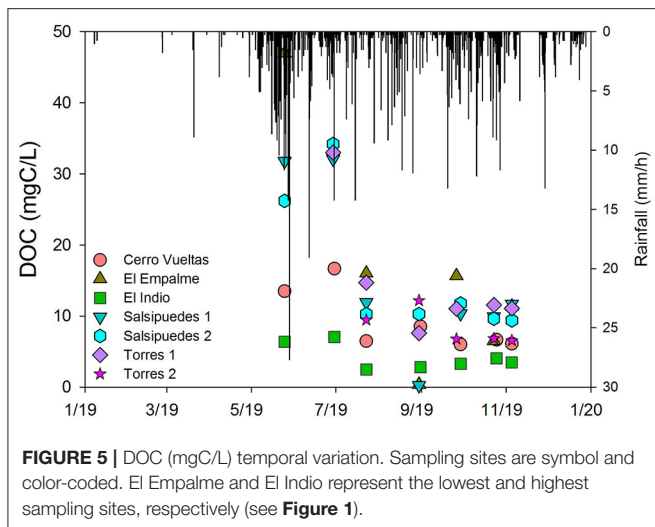
RESULTS AND DISCUSSION

Peat Bogs Water Chemistry

Figure 3 shows a summary of the main water chemistry characteristics across the study sites. Peat bogs exhibited low EC in the range of precipitation (from 5 to 35 μS/cm) with acidic conditions between 4 and 6 pH units (**Figures 3a,b**). Major ion concentrations were relative low (Cl^- < 3.5 mg/L; SO_4^{-2} < 4 mg/L; NO_3^- < 1.2 mg/L; Ca^{+2} < 2 mg/L), suggesting slow rock weathering rates and minimal anthropogenic effects (Markham and Otárola, 2021) (**Figures 3d–f**). Turbidity averaged ∼5 NTU across the hydrological year, with the exception of Torres 1 site (up to 30 NTU) (**Figure 3c**). Based on the water chemistry characteristics, the study sites are defined as ombrotrophic bogs (i.e., mainly fed by precipitation) (Lindsay, 2016).

DIC concentrations were below 2 mg/L and $\delta^{13}C_{DIC}$ compositions indicated a mixture between soil organic matter, soil CO_2, CO_2 in soil water, and in less degree DIC derived from bacterial CO_2 (mean $\delta^{13}C_{DIC}$ = −18.0 ± 4.7‰) (Pawellek and Veizer, 1994; Horgby et al., 2019) (**Figures 3i,j**). Water stable isotopes indicated a clear meteoric origin (Esquivel-Hernández et al., 2018, 2019, 2021) for this high elevation Páramo ecosystem, with $\delta^{18}O$ values ranging from −5.4 to −12.1‰, with a mean value of −9.2 ± 1.4‰. Similar to high elevation glacial lakes in this region (Esquivel-Hernández et al., 2018), the shallow peat bogs are also exposed to evaporation during the dry season (**Figures 3g, 4**). Deuterium excess values indicated evaporation losses during the dry season (down to −1.5‰) and moisture recycling during the rain events of the wet season (up to +15.7‰)

FIGURE 4 | Dual isotope diagram including peat bogs (pink squares) and rainfall (gray dots) during the 2019 hydrological year at the Páramo ecosystem. The local meteoric water line (LMWL) during 2019 (black line) is included as reference (Esquivel-Hernández et al., 2021).

(Sánchez-Murillo et al., 2020) (**Figure 3h**). During the dry season (December to April), the strengthening of the easterly trade winds (Amador, 1998) results in low intensity horizontal rainfall events (Bruijnzeel et al., 2010), which in turn maintain the peat bogs near saturation; while water logging occurs mainly from mid-May to the end of November.

FIGURE 5 | DOC (mgC/L) temporal variation. Sampling sites are symbol and color-coded. El Empalme and El Indio represent the lowest and highest sampling sites, respectively (see **Figure 1**).

Dissolved Carbon Content and Optical Properties

Figure 5 shows a temporal variation of DOC across all sites vs. rainfall amounts. During the wet season (mid-May to November), rainfall inputs are critical to sustain saturated soils and maintain anoxic conditions, which in turn exert a large control on carbon storage and humification processes. At the end of the dry season (April to mid-May), DOC concentrations were relative high across almost all the sites (up to ~50 mg/L). DOC concentrations were stabilized below ~15 mg/L as the rainy season progressed. Cerro Vueltas and El Indio sites (highest elevation sites; **Figure 1**) exhibited a rather uniform DOC pattern from July to November, with DOC values below 10 mg/L.

Figure 6 summarizes the dissolved carbon optical properties throughout the hydrological year. In general, ~91% of the dissolved carbon in the peat bogs corresponded to organic carbon. DOC concentrations ranged from 0.2 up to 47.0 mg/L (**Figure 6b**). Páramo DOC concentrations are relatively high when compared to other tropical water reservoirs. For example, Osburn et al. (2018) and Sánchez-Murillo et al. (2019) reported stream DOC concentrations ranging from 7.65 up to 11.52 mg/L, respectively, during storm events in swamp primary and secondary forests of the Caribbean slope of central Costa Rica. Williams et al. (2001) and Pesántez et al. (2018) reported mean DOC concentrations in Páramo wetlands and natural forests of the Ecuadorian Andes of 23.0 and 11.0 mg/L, respectively. Dalmagro et al. (2017) found significant DOC differences between the dry (~2 mg/L) and wet (~6 mg/L) seasons within the large Brazilian Pantanal wetland. Similarly, the authors reported greater DOC concentrations in forested areas than pasture regions. A global meta-analysis of DOC concentrations reported a mean value of 3.87 mg/L across South America river basins (Chaplot and Mutema, 2021).

El Indio site consistently reported low DOC concentrations and humic-like intensities, whereas protein-like intensity peaks were stronger than the rest of the peak bogs. Large DOC concentrations at El Empalme site (lower elevation and near

anthropogenic influence, see **Figure 1**) were consistently linked to humic-like intensity peaks C, A, and M (i.e., recalcitrant material) (Coble, 1996; Hansen et al., 2016) (**Figures 6e–g**). Protein-like intensity peaks (B and T) (better refer as fresh-like material) were particularly lower in Salsipuedes 2 and Torres 1 sites (**Figures 6h,i**).
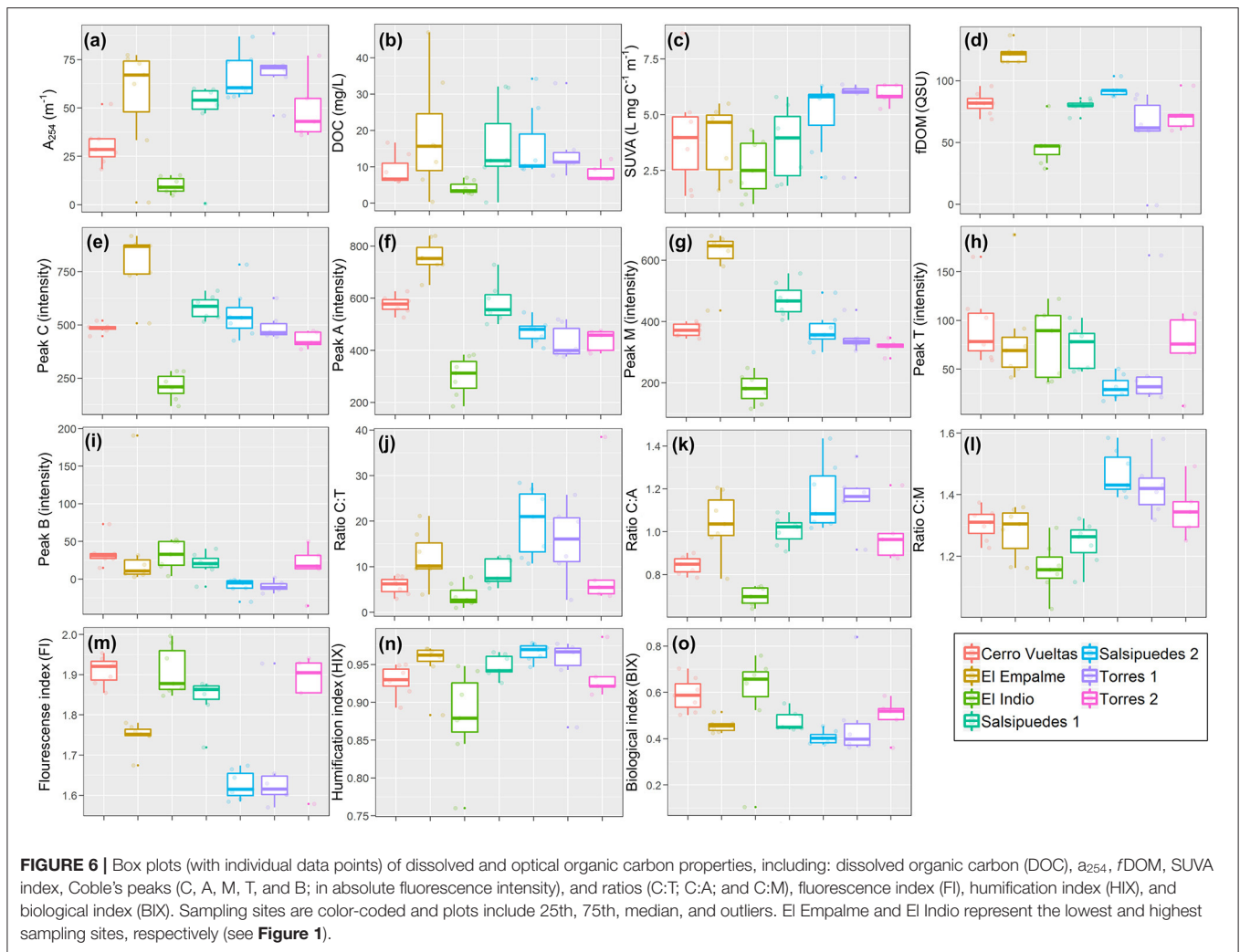
$SUVA_{254}$ is often related to hydrophobic organic acid fraction and constitutes a useful proxy of aromatic content and molecular weight of DOM (Weishaar et al., 2003). $SUVA_{254}$ values varied from 0.02 up to $8.72\,L\,mgC^{-1}\,m^{-1}$, with Salsipuedes 2 and Torres 1-2 sites exhibiting greater aromatic content than the rest of the peat bogs (**Figures 6a–c**). Despite the pristine nature of these high elevation peatbogs, it is important to remark that re-oxygenation of any reduced iron could lead to elevated absorbance (and thus $SUVA_{254}$ values) not linked to DOM absorbance (Poulin et al., 2014).

In general, the intensity of humic-like peaks was 6–7 times greater than fresh-like peaks across all sites. C:T ratios (an indication of the amount of degraded vs. fresh-like material) were greater at Salsipuedes 2 and Torres 1 (**Figure 6j**). Overall C:T ratios averaged 10.9, indicating a greater relative contribution of soil-derived DOM (Hansen et al., 2016). C:A ratios (an indication of the amount of humic-like vs. fulvic-like material) were <1 at three sites (Cerro Vueltas, El Indio, and Torres 2) indicating more prevalence of fulvic-like material (**Figure 6k**). C:M ratios at Salsipuedes 2 and Torres 1-2 sites exhibited greater values than the rest of the peat bogs, which in turn may suggest larger compositions of diagenetically altered material (microbial activity in sediments and soils) (**Figure 6l**).

The biological index (BIX) (an indication of autotrophic activity; Huguet et al., 2009) was below 1 across all sites (**Figure 6o**) indicating that DOM in the peat bogs was not recently produced. The latter clearly correspond to relative high values of humification (HIX; an indicator of humic substance content; Zsolnay et al., 1998) between 0.76 and 0.99. HIX values in natural waters range from 0.6 to 0.9 (Hansen et al., 2016) (**Figure 6n**). However, Dalmagro et al. (2017) have reported mean HIX values >10 whitin the large Brazilian Pantanal wetland. El Indio site exhibited the lower HIX values corresponding with low intensities in peaks C, A, and M (**Figure 6n**). The contribution of terrestrial to microbial sources to the DOM pool was evaluated with the fluorescence index (FI) (Mcknight et al., 2001). In natural water and tropical wetlands FI values ranged between 1.2 and 1.8 (Hansen et al., 2016; Dalmagro et al., 2017). In the peat bogs, FI values varied between 1.6 and 2.0, with a prevalence of microbial sources at Cerro Vueltas, El Indio, Salsipuedes 1, and Torres 2. FI values at Salsipuedes 2 and Torres 1 indicated a tendency toward more terrestrial DOM derived sources (**Figure 6m**).

Excitation/Emission Fluorescence Matrices (EEMs)

Based on the EEMs regions defined by wavelength boundaries (Chen et al., 2003 and references therein), El Empalme site exhibited strong intensities in a region dominated by humic acid-like substances (Region V), followed by a moderate intensity in

FIGURE 6 | Box plots (with individual data points) of dissolved and optical organic carbon properties, including: dissolved organic carbon (DOC), a_{254}, fDOM, SUVA index, Coble's peaks (C, A, M, T, and B; in absolute fluorescence intensity), and ratios (C:T; C:A; and C:M), fluorescence index (FI), humification index (HIX), and biological index (BIX). Sampling sites are color-coded and plots include 25th, 75th, median, and outliers. El Empalme and El Indio represent the lowest and highest sampling sites, respectively (see **Figure 1**).

the fulvic acid-like region (Region III), with minimal influence of protein or microbial by-product like contents (**Figure 7**). This is supported by strong C, A, and M peaks and high humification processes from terrestrial derived DOM (**Figures 6e–g**).

In contrast, El Indio and Torres 2 sites reported moderate intensities in Regions V-III, with also moderate signals in Regions I-II (i.e., aromatic proteins), corresponding to high FI and BIX values, and the lower HIX values. EEMs denoted a high prevalence of humic and fulvic acids in the peat bogs, with moderate to low intensities in soluble microbial by-product-like and aromatic proteins regions at Cerro Vueltas, El Indio, and Torres 2 (**Figure 7**).

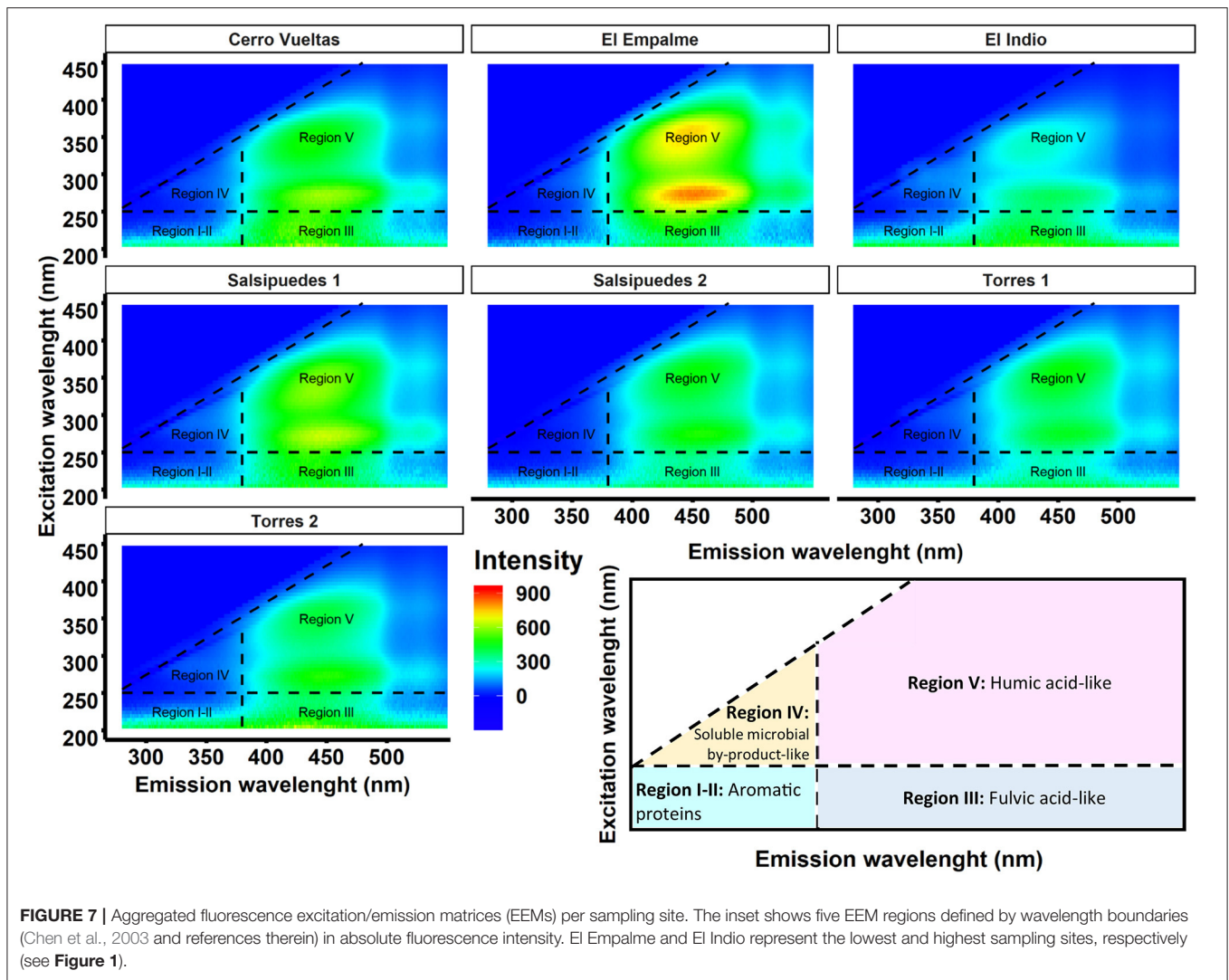## Exploring Water Chemistry and Dissolved Carbon Relationships

PCA dimensions 1 and 2 together explained 68.8% of the total variance in the data set (**Figure 8**). Dimension 1, which explained 48.5% of the total variance, showed strong positive loadings for variables associated with humification processes (e.g., peaks C, A,

and M; ratios, HIX, DOC, and a_{254}) and thus, fungal degraded by-products. On the other hand, dimension 2 which explained 20.4% of the total variance, showed positive loadings for parameters related with protein-like materials (peaks T and B), pH, and microbial derived DOM.

The PCA output also allowed the visualization of sampling sites within the framework of dimensions 1 and 2. El Empalme exhibited a high positive score on the dimension 1 axis, related with the presence of humic-like intensity peaks. Cerro Vueltas site showed a low positive score on the dimension 2, associated with microbial derived indexes (FI and BIX). Salsipuedes 2 and Torres 1 were related to humification ratios, whereas El Indio and Torres 2 were not related with a clear pattern between the PCA dimensions. Salsipuedes 1 was associated with moderate positive scores to humic-like and protein-like peaks.

CONCLUSIONS

Our study revealed that fluorescence intensity of humic-like peaks was 6–7 times greater than fresh-like peaks across all
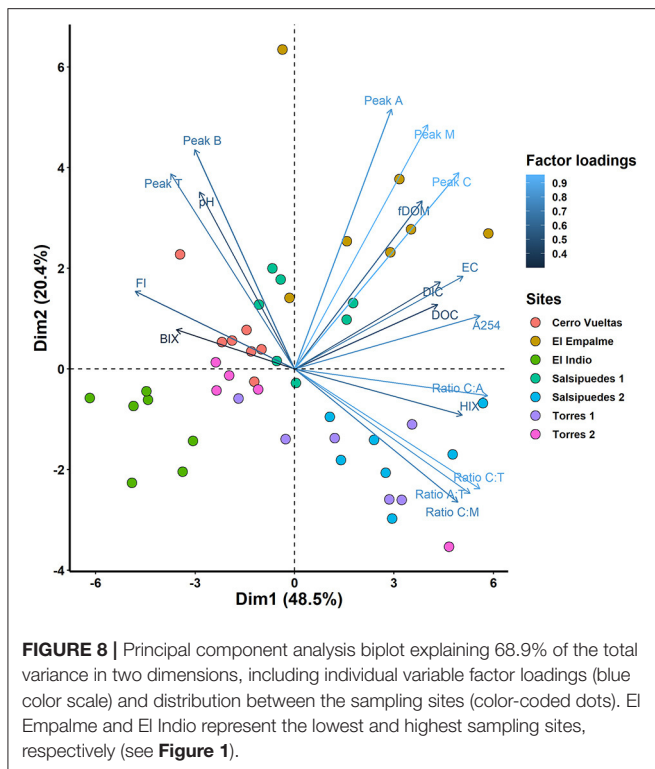
FIGURE 7 | Aggregated fluorescence excitation/emission matrices (EEMs) per sampling site. The inset shows five EEM regions defined by wavelength boundaries (Chen et al., 2003 and references therein) in absolute fluorescence intensity. El Empalme and El Indio represent the lowest and highest sampling sites, respectively (see **Figure 1**).

sites throughout a wet season. Second order indexes (BIX, and HIX) point to a greater relative contribution of recalcitrant soil-derived DOM with a high prevalence of humic and fulvic acids in the peat bogs. Evidence of fresh organic material from soluble microbial by-products and aromatic protein were detected in less degree, indicating also active microbial activity as a secondary decomposition pathway.

Our study comprises one exploratory sampling campaign during a complete hydrological year which limits the ability of exploring the impacts of inter-annual rainfall variability on DOC transport and export. However, from mid-May to the end of November, rainfall inputs are critical to sustain saturated soils, anoxic and acid conditions, which in turn exert a large control on carbon storage and humification processes. Our data revealed a clear seasonal pattern during the hydrological year. At the end of the dry season (April to mid-May), DOC concentrations were relatively high in almost all the sites. As the rainy season progressed, DOC concentrations decreased below 10 mg/L.

Since the Central America region has been experiencing recurrent droughts, it is expected that DOC concentrations may be significantly higher during post-drought events (enzymatic flush mechanism). Dry and oxic conditions reduces DOC decomposition due to the inhibitory effect of phenolic compounds on microbial activity (Fenner and Freeman, 2011). Our study also suggest that more robust sampling efforts using at higher temporal and spatial resolution using optical absorbance and fluorescence spectroscopic techniques (Dalmagro et al., 2017) are needed to underpin the potential impact of climate variability over DOM stocks, sources, and export, as well as microbial community changes between the dry and wet seasons (Stegen et al., 2016).

Further research on the relevance of photodegradation on temporal DOM dynamics of these highland peatbogs would also be of interest considering the high UV radiation to which the Páramo ecosystems are subjected to. Similarly, lowland drinking water operators should pay careful attention to DOM export (Osburn et al., 2018; Sánchez-Murillo et al., 2019), since high

FIGURE 8 | Principal component analysis biplot explaining 68.9% of the total variance in two dimensions, including individual variable factor loadings (blue color scale) and distribution between the sampling sites (color-coded dots). El Empalme and El Indio represent the lowest and highest sampling sites, respectively (see **Figure 1**).

DOC concentrations particularly after prolonged droughts, may act as a substrate for microbial growth and may react during chlorination to form disinfection byproducts in the resultant drinking water (Ritson et al., 2017).

DATA AVAILABILITY STATEMENT

The datasets presented in this study can be found in online repositories. The names of the repository/repositories and accession number(s) can be found below: https://doi.org/ 10.4211/hs.d001620c2f104a0891dc18825ea2fe31, CUAHSI (Sánchez-Murillo et al., 2021).

AUTHOR CONTRIBUTIONS

RS-M and PG-A conceived the presented idea. RS-M, MP, and PG-A carried out all field sampling campaigns. RS-M, RS-G, GE-H, and RP-S conducted all chemical analyses. RS-M and RS-G collaborated with R statistical tests. RS-M initiated the first manuscript draft. All authors contributed to the final manuscript version.

FUNDING

ACKNOWLEDGMENTS

SUPPLEMENTARY MATERIAL

The Supplementary Material for this article can be found online at: https://www.frontiersin.org/articles/10.3389/frwa. 2021.742780/full#supplementary-material

REFERENCES

Amador, J. A. (1998). A climatic feature of the tropical Americas: the trade wind easterly jet. *Top. Meteor. Oceanogr.* 5, 91–102.

APHA and AWWA (2005). *Standard Methods for the Examination of Water and Wastewater, 20, Federation*. Washington, DC: American Public Health Association/American Water Works Association/Water Environment.

Arriagada, R. A., Sills, E. O., Ferraro, P. J., and Pattanayak, S. K. (2015). Do payments payoff? *Evidence from participation in Costa Rica's PES program. PLoS ONE* 10:e0136809. doi: 10.1371/journal.pone.0136809

Berbés-Blázquez, M., Bunch, M. J., Mulvihill, P. R., Peterson, G. D., and de Joode, B. V. W. (2017). Understanding how access shapes the transformation of ecosystem services to human well-being with an example from Costa Rica. *Ecosyst. Serv.* 28, 320–327. doi: 10.1016/j.ecoser.2017.09.010

Bispo, D. F. A., Silva, A. C., Christofaro, C., Silva, M. L. N., Barbosa, M. S., Silva, B. P. C., et al. (2016). Hydrology and carbon dynamics of tropical peatlands from Southeast Brazil. *Catena* 143, 18–25. doi: 10.1016/j.catena.2016.03.040

Blair, R. C., Higgins, J. J., Karniski, W., and Kromrey, J. D. (1994). A study of multivariate permutation tests which may replace Hotelling's T2 test in prescribed circumstances. *Multivar. Behav. Res.* 29, 141–163. doi: 10.1207/s15327906mbr2902_2

Bourgeau-Chavez, L. L., Endres, S. L., Graham, J. A., Hribljan, J. A., Chimner, R. A., Lillieskov, E. A., et al. (2018). "Mapping peatlands in boreal and tropical ecoregions," in *Comprehensive Remote Sensing*, ed S. Liang (Oxford: Elsevier), 24–44. doi: 10.1016/B978-0-12-409548-9.10544-5

Brak, B., Vroklage, M., Kappelle, M., and Cleef, A. M. (2005). "Comunidades vegetales de la turbera de altura "La Chonta" en Costa Rica," in *Páramos de Costa Rica*, eds M. Kappelle and S. P. Horn (Costa Rica: Editorial INBio), 607–630.

Bruijnzeel, L. A., Scatena, F. N., and Hamilton, L. S. (2010). *Tropical Montane Cloud Forests: Science for Conservation and Management*. Cambridge: Cambridge University Press. doi: 10.1017/CBO97805117 78384

Chaplot, V., and Mutema, M. (2021). Sources and main controls of dissolved organic and inorganic carbon in river basins: a worldwide meta-analysis. *J. Hydrol.* 603:126941. doi: 10.1016/j.jhydrol.2021.126941

Chaves, R. C., Figueredo, C. C., Boëchat, I. G., de Oliveira, J. T. M., and Gücker, B. (2020). Fluorescence indices of dissolved organic matter as early warning

signals of fish farming impacts in a large tropical reservoir. *Ecol. Indic.* 115:106389. doi: 10.1016/j.ecolind.2020.106389

Chen, W., Westerhoff, P., Leenheer, J. A., and Booksh, K. (2003). Fluorescence excitation– emission matrix regional integration to quantify spectra for dissolved organic matter. *Environ. Sci. Technol.* 37, 5701–5710. doi: 10.1021/es034354c

Coble, P. G. (1996). Characterization of marine and terrestrial DOM in seawater using excitation-emission matrix spectroscopy. *Marine Chem.* 51, 325–346. doi: 10.1016/0304-4203(95)00062-3

Cook, S., Peacock, M., Evans, C. D., Page, S. E., Whelan, M. J., Gauci, V., et al. (2017). Quantifying tropical peatland dissolved organic carbon (DOC) using UV-visible spectroscopy. *Water Res.* 115, 229–235. doi: 10.1016/j.watres.2017.02.059

Cooper, D. J., Sueltenfuss, J., Oyague, E., Yager, K., Slayback, D., Cabero-Caballero, E. M., et al. (2019). Drivers of peatland water table dynamics in the central Andes, Bolivia and Peru. *Hydrol. Proc.* 33, 1913–1925, doi: 10.1002/hyp.13446

Cooper, D. J., Wolf, E. C., Colson, C., Vering, W., Granda, A., and Meyer, M. (2010). Alpine Peatlands of the Andes, Cajamarca, Peru. *Arctic Antarctic Alpine Res.* 42, 19–33, doi: 10.1657/1938-4246-42.1.19

Corrales Ulate, L. D. M. (2018). *Caracterización biofísica y determinación del intercambio de gases de efecto invernadero en las turberas de Talamanca, Costa Rica.* Available online at: http://201.207.189.89/handle/11554/8975

Couwenberg, J., Dommain, R., and Joosten, H. (2010). Greenhouse gas fluxes from tropical peatlands in Southeast Asia. *Glob. Change Biol.* 16, 1715–1732, doi: 10.1111/j.1365-2486.2009.02016.x

Craig, H. (1957). Isotopic standards for carbon and oxygen and correction factors for mass-spectrometric analysis of carbon dioxide. *Geochim. Cosmochim. Acta* 12, 133–149. doi: 10.1016/0016-7037(57)90024-8

Dalmagro, H. J., Johnson, M. S., de Musis, C. R., Lathuillière, M. J., Graesser, J., Pinto-Júnior, O. B., et al. (2017). Spatial patterns of DOC concentration and DOM optical properties in a Brazilian tropical river-wetland system, J. *Geophys. Res. Biogeosci.* 122, 1883–1902. doi: 10.1002/2017JG003797

Dansgaard, W. (1964). Stable isotopes in precipitation. *Tellus* 16, 436–468. doi: 10.3402/tellusa.v16i4.8993

Drake, T. W., Van Oost, K., Barthel, M., Bauters, M., Hoyt, A. M., Podgorski, D. C., et al. (2019). Mobilization of aged and biolabile soil carbon by tropical deforestation. *Nature Geosci.* 12, 541–546. doi: 10.1038/s41561-019-0384-9

Esquivel-Hernández, G., Mosquera, G. M., Sánchez-Murillo, R., Quesada-Román, A., Birkel, C., Crespo, P., et al. (2019). Moisture transport and seasonal variations in the stable isotopic composition of rainfall in Central American and Andean Páramo during El Niño conditions (2015–2016). *Hydrol. Proc.* 33,1802–1817. doi: 10.1002/hyp.13438

Esquivel-Hernández, G., Sánchez-Murillo, R., Quesada-Román, A., Mosquera, G. M., Birkel, C., and Boll, J. (2018). Insight into the stable isotopic composition of glacial lakes in a tropical alpine ecosystem: Chirripó, Costa Rica. *Hydrol. Proc.* 32, 3588–3603. doi: 10.1002/hyp.13286

Esquivel-Hernández, G., Sánchez-Murillo, R., and Vargas-Salazar, E. (2021). Chirripó hydrological research site: advancing stable isotope hydrology in the Central American Páramo. *Hydrol. Proc.* 35:e14181. doi: 10.1002/hyp.14181

Fenner, N., and Freeman, C. (2011). Drought-induced carbon loss in peatlands. *Nature Geosci.* 4, 895–900. doi: 10.1038/ngeo1323

Friendly, M. (2002). Corrgrams: Exploratory displays for correlation matrices. *Am. Stat.* 56, 316–324. doi: 10.1198/000313002533

Gandois, L., Teisserenc, R., Cobb, A. R., Chieng, H. I., Lim, L. B. L., Kamariah, A. S., et al. (2014). Origin, composition, and transformation of dissolved organic matter in tropical peatlands. *Geochim. Cosmochim. Acta* 137, 35–47, doi: 10.1016/j.gca.2014.03.012

Gómez, L. D. (1986). *Vegetación y Clima de Costa Rica.* San José: Editorial de la Universidad Estatal a Distancia.

Good, P. (2000). *Permutation Test: A Practical Guide to Resampling Methods for Testing Hypotheses,* 2nd ed., eds P. Bickel, P. Diggle, S. Fienberg, K. Krickeberg, I. Olkin, N. Wermuth, and S. Zeger. New York, NY: Springer. doi: 10.1007/978-1-4757-3235-1

Gröning, M., Lutz, H. O., Roller-Lutz, Z., Kralik, M., Gourcy, L., and Pöltenstein, L. (2012). A simple rain collector preventing water re-evaporation dedicated for δ^{18}O and δ^2H analysis of cumulative precipitation samples. *J. Hydrol.* 448, 195–200. doi: 10.1016/j.jhydrol.2012.04.041

Gumbricht, T., Roman-Cuesta, R. M., Verchot, L., Herold, M., Wittmann, F., Householder, E., et al. (2017). An expert system model for mapping tropical wetlands and peatlands reveals South America as the largest contributor. *Glob. Change Biol.* 23, 3581–3599. doi: 10.1111/gcb.13689

Hansen, A. M., Kraus, T. E., Pellerin, B. A., Fleck, J. A., Downing, B. D., and Bergamaschi, B. A. (2016). Optical properties of dissolved organic matter (DOM): effects of biological and photolytic degradation. *Limnol. Oceanogr.* 61, 1015–1032. doi: 10.1002/lno.10270

Hapsari, K. A., Biagioni, S., Jennerjahn, T. C., Meyer Reimer, P., Saad, A., Achnopha, Y., et al. (2017). Environmental dynamics and carbon accumulation rate of a tropical peatland in Central Sumatra, Indonesia. *Quat. Sci. Rev.* 169, 173–187, doi: 10.1016/j.quascirev.2017.05.026

Helsel, D. (2012). *Statistics for Censored Environmental Data Using Minitab® and R.* New Jersey, NY: John Wiley and Sons. doi: 10.1002/9781118162729

Horgby, Å., Segatto, P. L., Bertuzzo, E., Lauerwald, R., Lehner, B., Ulseth, A. J., et al. (2019). Unexpected large evasion fluxes of carbon dioxide from turbulent streams draining the world's mountains. *Nat. Commun.* 10, 1–9. doi: 10.1038/s41467-019-12905-z

Hribljan, J. A., Suárez, E., Heckman, K. A., Lilleskov, E. A., and Chimner, R. A. (2016). Peatland carbon stocks and accumulation rates in the Ecuadorian paramo. *Wetlands Ecol. Manag.* 24, 113–127, doi: 10.1007/s11273-016-9482-2

Huguet, A., Vacher, L., Relexans, S., Saubusse, S., Froidefond, J. M., and Parlanti, E. (2009). Organic geochemistry properties of fluorescent dissolved organic matter in the Gironde Estuary. *Org. Geochem.* 40, 706–719. doi: 10.1016/j.orggeochem.2009.03.002

Itoh, M., Okimoto, Y., Hirano, T., and Kusin, K. (2017). Factors affecting oxidative peat decomposition due to land use in tropical peat swamp forests in Indonesia. *Sci. Total Environ.* 609, 906–915. doi: 10.1016/j.scitotenv.2017.07.132

Jiménez, J. A. (2016). "Bogs, marshes, and swamps of Costa Rica," in *Costa Rican Ecosystems,* ed M. Kappelle (Chicago: University of Chicago Press), 866–894.

Kiew, F., Hirata, R., Hirano, T., Xhuan Wong, G., Baran Aeries, E., Kemudang Musin, K., et al. (2018). CO_2 balance of a secondary tropical peat swamp forest in Sarawak, Malaysia. *Agr. Forest Meteorology* 248, 494–501. doi: 10.1016/j.agrformet.2017.10.022

Kimmel, K., and Mander, Ü. (2010). Ecosystem services of peatlands: implications for restoration. *Progr. Phys. Geogr.* 34, 491–514. doi: 10.1177/0309133310365595

Lachniet, M. S., and Seltzer, G. O. (2002). Late quaternary glaciation of Costa Rica. *Geol. Society Am. Bull.* 114, 547–558. doi: 10.1130/0016-7606(2002)114<0547:LQGOCR>2.0.CO;2

Lê, S., Josse, J., and Husson, F. (2008). FactoMineR: a package for multivariate analysis. *J. Stat. Softw.* 25, 1–18. doi: 10.18637/jss.v025.i01

Leng, L. Y., Haruna Ahmed, O., and Boyie Jalloh, M. (2019). Brief review on climate change and tropical peatlands. *Geosci. Front.* 10:18, doi: 10.1016/j.gsf.2017.12.018

Li, W., Dickinson, R. E., Fu, R., Niu, G.-Y., Yang, Z.-L., and Canadell, J. G. (2007). Future precipitation changes and their implications for tropical peatlands. *Geophys. Res. Lett.* 34:L01403. doi: 10.1029/2006GL028364

Lindsay, R. (2016). *Peatland (Mire Types): Based on Origin and Behavior of Water, Peat Genesis, Landscape Position, and Climate.* Dordrecht: Springer Netherlands. doi: 10.1007/978-94-007-6173-5_279-1

Lourençato, L. F., Caldeira, P. P., Bernardes, M. C., Buch, A. C., Teixeira, D. C., and Silva-Filho, E. V. (2017). Carbon accumulation rates recorded in the last 150 years in tropical high mountain peatlands of the Atlantic Rainforest, SE – Brazil. *Sci. Total Environ.* 579, 439–446. doi: 10.1016/j.scitotenv.2016.11.076

Markham, J., and Otárola, M. F. (2021). Bryophyte and lichen biomass and nitrogen fixation in a high elevation cloud forest in Cerro de La Muerte, Costa Rica. *Oecologia* 195, 489–497. doi: 10.1007/s00442-020-04840-4

Marx, A., Dusek, J., Jankovec, J., Sanda, M., Vogel, T., van Geldern, R., et al. (2017). A review of CO_2 and associated carbon dynamics in headwater streams: a global perspective. *Rev. Geophysics* 55, 560–585. doi: 10.1002/2016RG000547

Mcknight, D. M., Boyer, E. W., Westerhoff, P. K., Doran, P. T., Kulbe, T., and Andersen, D. T. (2001). Spectrofluorometric characterization of dissolved organic matter for indication of precursor organic material and aromaticity. *Limnol. Oceanogr.* 46, 38–48. doi: 10.4319/lo.2001.46.1.0038

Moore, S., Evans, C. D., Page, S. E., Garnett, M. H., Jones, T. G., Freeman, C., et al. (2013). Deep instability of deforested tropical peatlands revealed by fluvial organic carbon fluxes. *Nature* 493, 660–664, doi: 10.1038/nature11818

Müller, D., Warneke, T., Rixen, T., Müller, M., Jamahari, S., Denis, N., et al. (2015). Lateral carbon fluxes and CO_2 outgassing from a tropical peat-draining river. *Biogeosciences* 12, 5967–5979. doi: 10.5194/bg-12-5967-2015

Osburn, C. L., Oviedo-Vargas, D., Barnett, E., Dierick, D., Oberbauer, S. F., and Genereux, D. P. (2018). Regional groundwater and storms are hydrologic controls on the quality and export of dissolved organic matter in two tropical rainforest streams, Costa Rica. *J. Geophys. Res.* 123, 850–866. doi: 10.1002/2017JG003960

Page, S. E., and Baird, A. J. (2016). Peatlands and global change: response and resilience. *Ann. Rev. Environ. Resourc.* 41, 35–57. doi: 10.1146/annurev-environ-110615-085520

Page, S. E., Siegert, F., Rieley, J. O., Boehm, H. D., Jaya, A., and Limin, S. (2002). The amount of carbon released from peat and forest fires in Indonesia during 1997. *Nature* 420, 61–65, doi: 10.1038/nature01131

Park, M., and Snyder, S. (2018). Sample handling and data processing for fluorescent excitation-emission matrix (EEM) of dissolved organic matter (DOM). *Chemosphere* 193, 530–537. doi: 10.1016/j.chemosphere.2017.11.069

Pawellek, F., and Veizer, J. (1994). Carbon cycle in the upper Danube and its tributaries: $\delta^{13}C_{DIC}$ constrains. *Israel J. Earth Sci.* 43, 187–194.

Pesántez, J., Mosquera, G. M., Crespo, P., Breuer, L., and Windhorst, D. (2018). Effect of land cover and hydro-meteorological controls on soil water DOC concentrations in a high-elevation tropical environment. *Hydrol. Proc.* 32, 2624–2635. doi: 10.1002/hyp.13224

Poulin, B. A., Ryan, J. N., and Aiken, G. R. (2014). Effects of iron on optical properties of dissolved organic matter. *Environ. Sci. Technol.* 48, 10098–10106. doi: 10.1021/es502670r

Pucher, M., Wünsch, U., Weigelhofer, G., Murphy, K., Hein, T., and Graeber, D. (2019). staRdom : versatile software for analyzing spectroscopic data of dissolved organic matter in R. *Water* 11, 1–19. doi: 10.3390/w11112366

R., Core Team (2019). *R: A Language and Environment for Statistical Computing.* Vienna: R Foundation for Statistical Computing. Available online at: https://www.R-project.org/ (accessed June 14, 2021).

Ribeiro, K., Pacheco, F. S., Ferreira, J. W., de Sousa-Neto, E. R., Hastie, A., Krieger Filho, G. C., et al. (2021). Tropical peatlands and their contribution to the global carbon cycle and climate change. *Glob. Change Biol.* 27, 489–505. doi: 10.1111/gcb.15408

Ritson, J. P., Brazier, R. E., Graham, N. J. D., Freeman, C., Templeton, M. R., and Clark, J. M. (2017). The effect of drought on dissolved organic carbon (DOC) release from peatland soil and vegetation sources. *Biogeosciences* 14, 2891–2902. doi: 10.5194/bg-14-2891-2017

Sánchez-Murillo, R., Esquivel-Hernández, G., Birkel, C., Correa, A., Welsh, K., Durán-Quesada, A. M., et al. (2020). Tracing water sources and fluxes in a dynamic tropical environment: from observations to modeling. *Front. Earth Sci* 8:571477. doi: 10.3389/feart.2020.571477

Sánchez-Murillo, R., Gastezzi, P., Sánchez-Gutiérrez, R., Esquivel-Hernández, G., and Pérez-Salazar, R. (2021). Optical properties of dissolved carbon in a high elevation tropical peatland ecosystem, *HydroShare.* doi: 10.4211/hs.d001620c2f104a0891dc18825ea2fe31

Sánchez-Murillo, R., Romero-Esquivel, L. G., Jiménez-Antillón, J., Salas-Navarro, J., Corrales-Salazar, L., Álvarez-Carvajal, J., et al. (2019). DOC transport and export in a dynamic tropical catchment. *J. Geophys. Res.* 124, 1665–1679. doi: 10.15359/cicen.1.35

Silva, A. C., Barbosa, M. S., Barral, U. M., Silva, B. P. C., Fernandes, J. S. C., Viana, A. J. S., et al. (2019). Organic matter composition and paleoclimatic changes in tropical mountain peatlands currently under grasslands and forest clusters. *Catena* 180, 69–82. doi: 10.1016/j.catena.2019.04.017

Spearman, C. E. (1904). The proof and measurement of association between two things. *Am. J. Psychol.* 15, 72–101. doi: 10.2307/1412159

Stan, K., and Sanchez-Azofeifa, A. (2019). Deforestation and secondary growth in Costa Rica along the path of development. *Reg. Environ. Change* 19, 587–597. doi: 10.1007/s10113-018-1432-5

Stegen, J. C., Fredrickson, J. K., Wilkins, M. J., Konopka, A. E., Nelson, W. C., Arntzen, E. V., et al. (2016). Groundwater–surface water mixing shifts ecological assembly processes and stimulates organic carbon turnover. *Nat. Commun.* 7:11237. doi: 10.1038/ncomms11237

Villa, J. A., Mejía, G. M., Velásquez, D., Botero, A., Acosta, S. A., Marulanda, J. M., et al. (2019). Carbon sequestration and methane emissions along a microtopographic gradient in a tropical Andean peatland. *Sci. Total Environ.* 654, 651–661, doi: 10.1016/j.scitotenv.2018.11.109

Waldron, S., Vihermaa, L., Evers, S. , Garnett, M. H., Newton, J., and Henderson, A. C. G. (2019). C mobilisation in disturbed tropical peat swamps: old DOC can fuel the fluvial efflux of old carbon dioxide, but site recovery can occur. *Sci. Rep.* 9:11429. doi: 10.1038/s41598-019-46534-9

Wallbott, L., G., and Siciliano, and Lederer, M. (2019). Beyond PES and REDD+: Costa Rica on the way to climate-smart landscape management? *Ecol. Soc.* 24:24. doi: 10.5751/ES-10476-240124

Wei, T., and Simko, V. (2021). *R package 'corrplot': Visualization of a Correlation Matrix. (Version 0.90).* Available online at: https://github.com/taiyun/corrplot (accessed June 14, 2021).

Weishaar, J. L., Aiken, G. R., Bergamaschi, B. A., Fram, M. S., Fujii, R., and Mopper, K. (2003). Evaluation of specific ultraviolet absorbance as an indicator of the chemical composition and reactivity of dissolved organic carbon. *Environ. Sci. Technol.* 37, 4702–4708. doi: 10.1021/es030360x

Williams, M. W., Hood, E. W., Ostberg, G., Francou, B., and Galarraga, R. (2001). Synoptic survey of surface water isotopes and nutrient concentrations, Páramo high-elevation region, Antisana Ecological Reserve, Ecuador. *Arctic Antarctic Alpine Res.* 33, 397–403. doi: 10.1080/15230430.2001.12003447

Yu, Z. (2011). Holocene carbon flux histories of the world's peatlands: Global carbon-cycle implications. *Holocene* 21, 761–774, doi: 10.1177/0959683610386982

Zsolnay, A., Baigar, E., and Jimenez, M. (1998). Differentiating with fluorescence spectroscopy the sources of dissolved organic matter in soils subjected to drying. *Chemosphere* 38, 45–50. doi: 10.1016/S0045-6535(98)00166-0